The 8th International Conference for Conveying and Handling of Particulate Solids
Tel-Aviv, Israel, May 2015

MACROSCOPIC BULK COHESION AND TORQUE FOR WET GRANULAR MATERIALS

S. Roy, S. Luding, and T. Weinhart

Faculty of Engineering Technology, MESA+, University of Twente,
P. O. Box 216, 7500 AE Enschede, The Netherlands

Abstract - Wet granular materials in steady-state in a quasi-static flow have been studied with discrete particle simulations. The total torque is an experimentally accessible macroscopic quantity that can be used to investigate the shear strength, bulk cohesion and other properties of the materials. We report in this paper how the macroscopic bulk cohesion and torque required to rotate the system change with the liquid content. Consequently, micro-macro correlations are obtained for the macro properties as a function of the microscopic liquid bridge volume which is one factor dominating the contact force.

1. INTRODUCTION

The strength, cohesion and flow properties of granular materials are strongly influenced by the presence of capillary cohesion. For example, sand castles with a small amount of water between the grains keep standing, with stable vertical walls, whereas sand castles built out of dry sand grains collapse and form a pile with a much smaller angle of repose. Due to the cohesive properties of the wet materials, the yield shear stress increases and as a result the partially saturated wet materials require higher torque for deformation (shear) *e.g.* by rotation in the shear cell. Efforts have been made to understand the effect of liquid bridge volume on different macroscopic properties like bulk cohesion or shear band properties [13]. In this paper we describe the calculation of the total torque required to shear the system for a given rotation rate. The torque is calculated from the microscopic forces of contact between the particles and walls of the shear cell. In the shear cell geometry under the condition of slow shear, the relative motion is confined to particles in a narrow region of high strain rate called the shear band [14]. Recent experimental studies show also that liquid is transported away from the shear band region [9, 10]. Here we study the effects with homogeneous liquid bridge volume throughout the system.

Earlier studies show that the macroscopic bulk cohesion increases non-linearly with increase in liquid bridge volume [3, 11, 12, 13] in the pendular liquid bridge regime. In this paper we study the effect of varying liquid bridge volume on the macroscopic torque required for rotation of the system. Many real life examples show that the bulk cohesion of the materials and the torque are closely related. Thus, we may ask, can we relate these two quantities from our numerical simulations to the microscopic forces due to the liquid bridges? In this paper we present the relation between the macro parameters (bulk cohesion and torque) and liquid bridge volume.

2. DISCRETE ELEMENT METHOD SIMULATION

We study the micro-macro relation for wet granular materials in the quasistatic regime with the Discrete Element Method using the open-source package MercuryDPM [15, 16]. In a shear cell geometry [2], the system consists of an outer cylinder (radius $R_o = 110$ mm) rotating with a frequency of $f_{rot} = 0.01$ s^{-1} around a fixed inner cylinder (radius $R_i = 14.7$ mm). The granular materials are confined between the two concentric cylinders, a bottom plate, and a free top surface by gravity . The bottom plate is split at radius $R_s = 85$ mm into a moving outer part and a static inner part. While in our previous work [12] and more [7, 8, 14], the simulations were done using a quarter of the system ($0\,^\circ \leq \psi \leq 90\,^\circ$), using periodic boundary conditions, in order to save computation time, here we simulate only a 30° section of the system ($0\,^\circ \leq \psi \leq 30\,^\circ$).

The numerical solutions of Newton's equations of motion is based on the specification of particle properties. The simulation details and the material parameters used in this study are the same as our previous work [12]. In order to study the influence of liquid content on the macroscopic torque, we analyzed the system for the following set of liquid bridge volumes V_b:

$$V_b \in [0,\ 1,\ 2,\ 4.2,\ 8,\ 14,\ 20,\ 75,\ 140,\ 200]\ \text{nl}, \tag{1}$$

which are all within the dry and pendular regime for our particles of mean diameter $d_p \approx 2.2$ mm. We use linear elastic contact model with a constant adhesive force due to the liquid bridge when the particles are in contact. The parameters of the contact model are particle stiffness $k = 120$ Nm^{-1}, viscous dissipation coefficient $\gamma_o = 0.5{\times}10^{-3}$ kgs^{-1}.

3. CAPILLARY BRIDGE FORCE MODEL

For wet granular materials with low saturation level, the particles are connected by individual capillary bridges. This regime is defined as the pendular regime. It exists approximately with bridge volumes between 0 to 300 nl, given the present particle sizes. The exact capillary force as a function

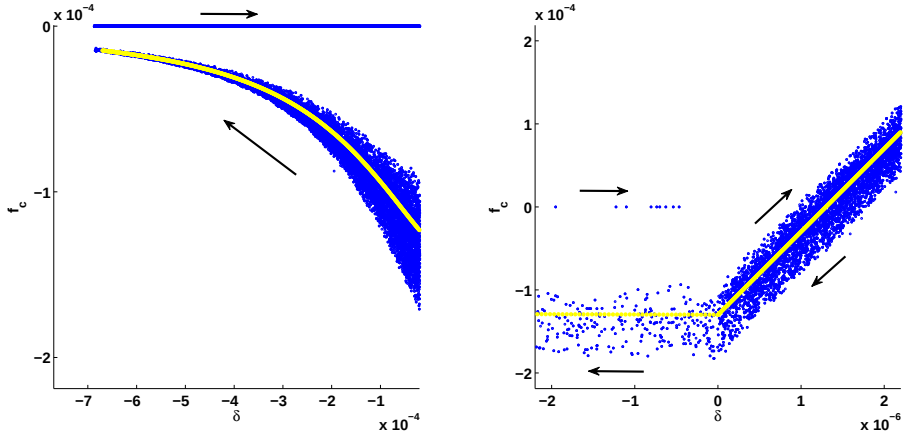

Figure 1: Liquid capillary bridge model for the (a) non-contact and (b) contact forces. The yellow lines represent the force for mean particle diameter d_p.

of separation distance can be calculated by numerically solving the Laplace - Young equation. We approximate the inter-particle capillary force f_c according to the proposal of [17] by:

$$f_c = \frac{2\pi\gamma r\cos\theta}{1 + 1.05\bar{S} + 2.5\bar{S}^2}, \tag{2}$$

where the separation distance is normalised as $\bar{S} = S\sqrt{(r/V_b)}$, S being the separation distance. The other parameters of the liquid capillary bridge model are contact angle $\theta = 20\,^\circ$ and surface tension of liquid $\gamma = 0.020\ \mathrm{Nm}^{-1}$ which closely corresponds to the surface tension of isopropanol. The effective radius of two spherical particles of different size can be estimated as the harmonic mean of the two particle radii according to the Derjaguin approximation [1], yielding the effective radius:

$$r = \frac{2r_i r_j}{r_i + r_j}, \tag{3}$$

This model equation was introduced for mono-disperse particles, and extended to poly-disperse system of particles in this paper Ref. [4]. There is no adhesive force acting between the particles during approach as the liquid bridge only forms once the particles contact each other; the adhesive force starts acting once they are in contact and remains constant during contact, $S \leq 0$. Once the particles separate, $S > 0$, the adhesive force is given by (2). The critical separation distance S_c between the particles before rupture is given as proposed by [5]:

$$S_c = \left(1 + \frac{\theta}{2}\right) V_b^{1/3}. \tag{4}$$

Figure 1 shows the liquid bridge forces as a function of the overlap δ for all contacts in the system.

4. MICRO MACRO TRANSITION

4.1 Macroscopic bulk cohesion

To extract the macroscopic fields, we use the spatial coarse-graining approach as given in [6, 7, 8]. In earlier studies [7, 8, 12, 13], shear band region was identified by the criterion of large strain rate, higher than a critical strain rate of $0.08\ \mathrm{s}^{-1}$. In this paper, the shear band region is defined by strain rates higher 80% of the maximum for different heights in the shear cell. When plotting the yield stress τ for the particles in the shear band region as a function of total pressure P (not shown), a linear trend is observed neglecting the different behavior for data at very low pressure (<100 Pa). This is fitted well by a linear function,

$$\tau = \mu P + c, \tag{5}$$

where μ is the macroscopic friction coefficient approximately equal to 0.15 as obtained from fitting and c is the macroscopic bulk cohesion. For non-cohesive systems, the macroscopic bulk cohesion is zero. As the volume of the liquid bridges increases, the yield shear stress increases and an offset is observed [3, 11, 12, 13]. Earlier studies show that the macroscopic bulk cohesion increases non-linearly with increase in liquid bridge volume [11, 12]. This is confirmed in Figure 2a, which shows that the macroscopic bulk cohesion as a function of liquid bridge volume for surface tension γ is well approximated by

$$c = c_o + a{V_b}^{1/3}, \tag{6}$$

where $c_o = 1.045$ Pa is the macroscopic bulk cohesion for $V_b = 0$ nl and $a = 1.179 \times 10^4\ \mathrm{Pa.m}^{-1}$. Eq. (4) shows that the rupture distance S_c is a cubic root function of the liquid bridge volume V_b. So figure 2a can be simplified as shown in figure 2b, the macroscopic cohesive strength as a function of the rupture distance S_c for surface tension γ, given by:

$$c = c_o + a' S_c, \tag{7}$$

where $a' = 1.004 \times 10^4\ \mathrm{Pa.m}^{-1}$.

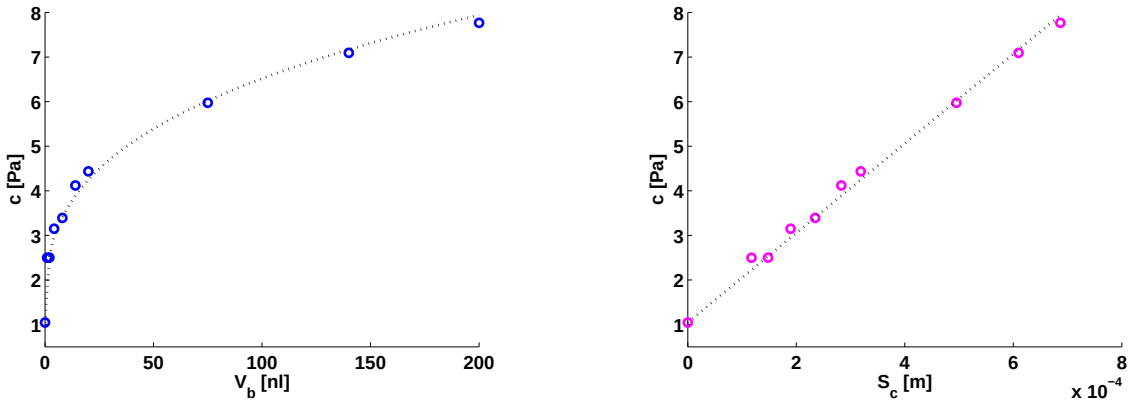

(a) (b)

Figure 2: Bulk cohesion as a function of a) liquid bridge volume V_b and b) rupture distance S_c for the given surface tension of liquid γ and contact angle θ. The dotted lines in the figure (a) and (b) are given by the fitting functions in Eq. (6) and (7) respectively.

4.2 Torque in a shear cell

The walls and the bottom plates of the shear cell consist of particles with a prescribed position. The particles forming the inner wall are stationary while the particles forming the outer wall rotate around the z-axis with frequenty f_{rot}. All the particles forming the inner and outer wall are identified as C_{inner} and C_{outer}, respectively. Figure 3 shows the wall particles on the moving outer part (magenta)

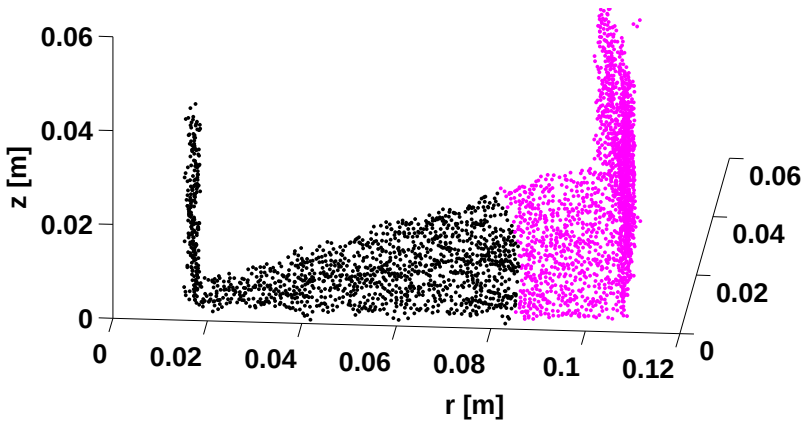

Figure 3: Particles involved in torque calculation, fixed particles attached on the moving wall and the base plate (magenta) and fixed particles attached on the fixed wall and the base plate (black) of the shear cell.

and the stationary inner part (black) of the shear cell. The macroscopic torque is calculated based on the contact forces on the attached particles on the moving part (outer) and stationary part (inner) of the shear cell. Thus the net inner and outer torque are calculated by summing up the torques for all the contacts with respect to the axis of rotation of the shear cell. The net torque is obtained from the difference between the outer wall torque and the inner wall torque. We multiply the total torque by a factor of $(2\pi)/(\pi/6)$ in order to get the torque for the whole system from the obtained torque of our simulations in its 30° section. Thus the global torque is given by:

$$\vec{T} = \frac{2\pi}{\pi/6}\Big[\Big(\sum_{i=1}^{N}\sum\nolimits_{j\in C_{\text{outer}}} \vec{c}_{i,j}\times\vec{f}_{i,j}\Big) - \Big(\sum_{i=1}^{N}\sum\nolimits_{j\in C_{\text{inner}}} \vec{c}_{i,j}\times\vec{f}_{i,j}\Big)\Big], \tag{8}$$

where N represents the number of particles, $\vec{c}_{i,j}$ is the position vector of the contact point and $\vec{f}_{i,j}$ is the interaction force. Only the z-component of the torque vector T^z is of interest as required for shearing the cell in angular direction.

Figure 4a shows the torque as a function of the liquid bridge volume. As the torque shows the same functional relation to the liquid bridge volume as the macroscopic bulk cohesion in (6), the fitting line in figure 4a is given by

$$T^z = T^z_o + bV_b{}^{1/3}, \tag{9}$$

where $T^z{}_o = 0.1248$ Nm is the torque for $V_b = 0$ nl and $b = 33.46$ N. Figure 4b shows macroscopic torque as a function of rupture distance S_c as given by:

$$T^z = T^z_o + b'S_c, \tag{10}$$

where $b' = 28.49$ N.

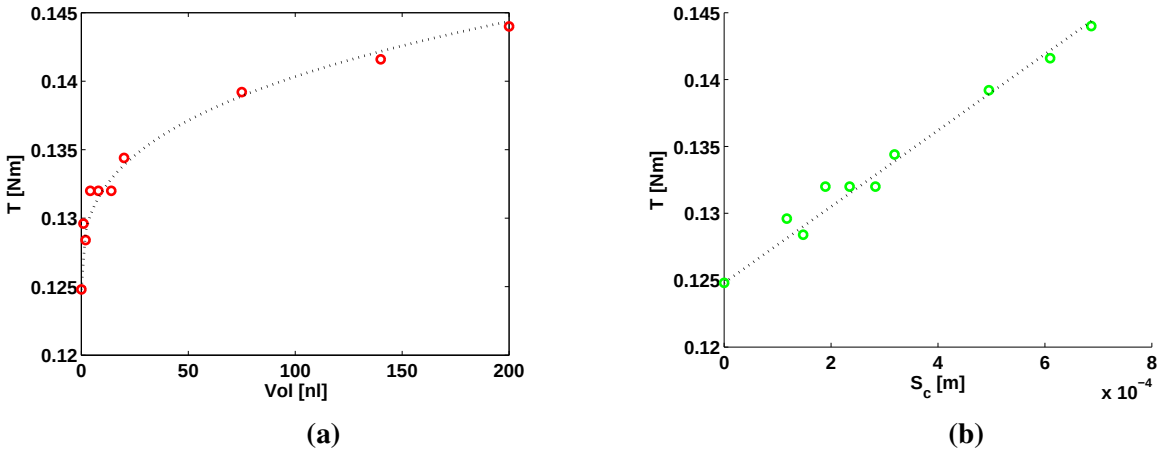

Figure 4: Macroscopic torque as a function of a) liquid bridge volume V_b and b) rupture distance S_c for the given surface tension of liquid γ and contact angle θ. The dotted lines in the figure (a) and (b) are given by the fitting functions in Eq. (9) and (10) respectively.

4.3 Correlation between macroscopic bulk cohesion and torque

The shear stress in the shear band is given by Eq. (5). Assuming the average shear stress on the inner wall and outer wall is proportional to shear stress in the shear band, the mean wall shear stress is given by $\tau_w = c'\tau$, where c' is a proportionality constant. Consequently, the scalar form of torque calculated on the wall is given by:

$$T^z_{macro} = c'\left[\int_{A_o} r\,dA - \int_{A_i} r\,dA\right](\mu P_{avg} + c), \tag{11}$$

where A_o denotes the surface of the outer wall, A_i denotes the surface of the inner wall, P_{avg} is the mean pressure inside the shear band approximately 250 Pa for a filling height of 39 mm. Eq. (11) can be simplified to the form:

$$T^z_{macro} = c'M(\mu P_{avg} + c), \tag{12}$$

where $M = \left[2\pi H(R_o{}^2 - R_i{}^2) + \frac{2}{3}\pi(R_o{}^3 + R_i{}^3 - 2R_s{}^3)\right] \approx 0.0031\,\mathrm{m}^3$ for the given geometry. Figure 5 shows the z - component of torque as given by Eq. (8) and T^z_{macro} as given by Eq. (12), for $c' \approx 1.03$, given as a function of the rupture distance S_c.

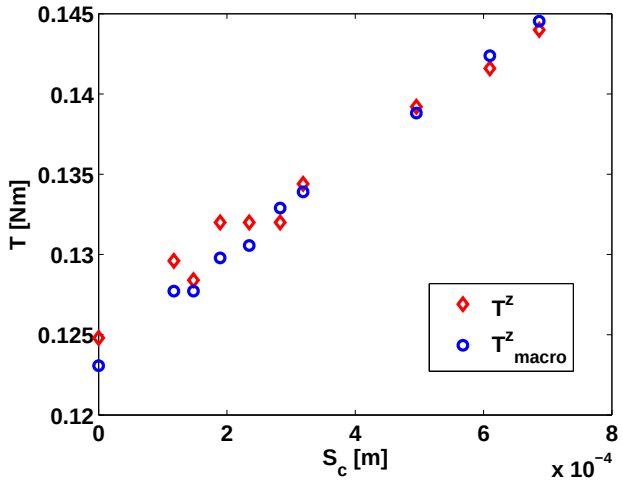

Figure 5: Comparison of macroscopic torque a)T^z and b)T^z_{macro} as given by Eq. (12) for $c' \approx 1.03$ as a function of the rupture distance S_c.

It is observed that the numerically calculated torque obtained from the summation of each contact force torque is comparable with the torque obtained from the average shear stress on the wall which is obtained from the macroscopic bulk cohesion as shown in above equation.

5. CONCLUSION

We performed simulations for different liquid content to study the effect of liquid bridge volume on bulk cohesion and torque of the system (certain other liquid properties like the surface tension and the contact angle are kept constant for all simulations). Both macro quantities increase with liquid content in the system, proportional to the third root of the liquid bridge volume, i.e. linear with the rupture distance of the liquid bridge. We compared the torque calculated from the average shear stress on the wall as obtained from the macroscopic bulk cohesion with the numerically calculated torque and found them comparable. This establishes the correlation between the (measured) torque and the macroscopic bulk cohesion.

In future work, the micro-macro correlation needs to be fully understood by studying the effect of other micro parameters on the macro behavior. This includes the effect of surface tension and contact angle of the liquid on the macroscopic bulk cohesion. Our goal is also to better understand the distribution of forces in their network and why that leads to the non-linear increase in bulk cohesion with increase in liquid bridge volume or, respectively, the linearity with rupture distance. Furthermore, the continuum stress at the walls should be computed from the simulations and used to predict the torque in order to complete the picture.

6. NOMENCLATURE

δ	Overlap [m]
V_b	Liquid bridge volume [nl]
θ	Contact angle [°]
γ	Surface tension of liquid [Nm^{-1}]
r	Mean radius [m]
f_c	Liquid bridge capillary force [N]

S	Inter-particle distance [m]
S_c	Rupture distance [m]
τ	Yield shear stress [Pa]
μ	Macroscopic friction coefficient
P_{avg}	Mean pressure inside the shear band [Pa]
c	Macroscopic bulk cohesion [Pa]
T	Torque [N.m]
R_i	Inner radius of shear cell [m]
R_o	Outer radius of shear cell [m]
R_s	Split radius of shear cell [m]
H	Filling height [m]

7. ACKNOWLEDGEMENTS

We acknowledge our financial support through STW project 12272 "Hydrodynamic theory of wet particle systems: Modeling, simulation and validation based on microscopic and macroscopic description."

8. REFERENCES

[1] Boris Deryaguin. Untersuchungen über die Reibung und Adhäsion, iv, Theorie des Anhaftens kleiner Teilchen, 1934.

[2] Denis Fenistein and Martin van Hecke. *Nature*, 425(6955):256, 2003.

[3] Anton Gladkyy and Rüdiger Schwarze. Comparison of different capillary bridge models for application in the discrete element method. *Granular Matter*, 16(6):911–920, 2014.

[4] Stephan Herminghaus. Dynamics of wet granular matter. *Advances in Physics*, 54(3):221–261, 2005.

[5] Guoping Lian, Colin Thornton, and Michael J Adams. A theoretical study of the liquid bridge forces between two rigid spherical bodies. *Journal of colloid and interface science*, 161(1):138–147, 1993.

[6] Stefan Luding. From microscopic simulations to macroscopic material behavior. *Computer Physics Communications*, 147(1):134–140, 2002.

[7] Stefan Luding. The effect of friction on wide shear bands. *Particulate Science and Technology*, 26(1):33–42, 2007.

[8] Stefan Luding. Constitutive relations for the shear band evolution in granular matter under large strain. *Particuology*, 6(6):501–505, 2008.

[9] Roman Mani, Dirk Kadau, and Hans J Herrmann. Liquid migration in sheared unsaturated granular media. *Granular Matter*, 15(4):447–454, 2013.

[10] Roman Mani, Dirk Kadau, Dani Or, and Hans J Herrmann. Fluid depletion in shear bands. *Physical review letters*, 109(24):248001, 2012.

[11] Vincent Richefeu, Moulay Saïd El Youssoufi, and Farhang Radjaï. Shear strength of unsaturated soils: Experiments, dem simulations, and micromechanical analysis. In *Theoretical and Numerical Unsaturated Soil Mechanics*, pages 83–91. Springer, 2007.

[12] Sudeshna Roy, Stefan Luding, and Thomas Weinhart. Towards hydrodynamic simulations of wet particles system. *Procedia Engineering*, accepted in 2014.

[13] Rüdiger Schwarze, Anton Gladkyy, Fabian Uhlig, and Stefan Luding. Rheology of weakly wetted granular materials: a comparison of experimental and numerical data. *Granular matter*, 15(4):455–465, 2013.

[14] Abhinendra Singh, Vanessa Magnanimo, Kuniyasu Saitoh, and Stefan Luding. Effect of cohesion on shear banding in quasistatic granular materials. *Physical Review E*, 90(2):022202, 2014.

[15] Anthony Thornton, Thomas Weinhart, Stefan Luding, and Onno Bokhove. Modeling of particle size segregation: calibration using the discrete particle method. *International Journal of Modern Physics C*, 23(08), 2012.

[16] Thomas Weinhart, Anthony R Thornton, Stefan Luding, and Onno Bokhove. From discrete particles to continuum fields near a boundary. *Granular Matter*, 14(2):289–294, 2012.

[17] Christopher D Willett, Michael J Adams, Simon A Johnson, and Jonathan PK Seville. Capillary bridges between two spherical bodies. *Langmuir*, 16(24):9396–9405, 2000.